

Spectral classification of emission-line galaxies

M. Dessauges-Zavadsky¹, M. Pindao¹, A. Maeder¹, and D. Kunth²

¹ Observatoire de Genève, 1290 Sauverny, Switzerland

² Institut d'Astrophysique de Paris, 98 bis Boulevard Arago, 75014 Paris, France

Received 24 June 1999/ Accepted 3 January 2000

Abstract. The main goal of this work is to further investigate the classification of emission-line galaxies from the “Spectrophotometric Catalogue of H II galaxies” by Terlevich et al. (1991) in a homogeneous and objective way, using the three line-ratio diagrams, called *diagnostic* diagrams, of Veilleux & Osterbrock (1987).

On the basis of the resulting catalogue, we critically discuss the classification methods in the optical range. In particular we compare our classification scheme to the one done by Rola et al. (1997) which is efficient for the classification of redshifted galaxies. We also propose a new diagnostic diagram involving the known intensity ratio $R_{23} = ([\text{O II}] \lambda 3727 + [\text{O III}] \lambda 4959 + [\text{O III}] \lambda 5007) / \text{H}\beta$ which appears to be a very good criterion allowing to discriminate the Seyfert 2 from H II galaxies.

The revised catalogue including 314 narrow-emission-line galaxies¹ contains H II galaxies, Seyfert 2 galaxies, Low Ionization Nuclear Emission-Line Regions (hereafter LINERs) galaxies and some particular types of galaxies with the most intriguing ones, called “ambiguous”, due to the ambiguity of their location in the diagnostic diagrams. These galaxies appear as H II galaxies and as active galactic nuclei (hereafter AGNs) in different diagrams of Veilleux & Osterbrock and constitute certainly a sample of particularly interesting candidates for a thorough study of connections between starbursts and AGNs.

Key words: catalogs – ISM: H II regions – galaxies: active – galaxies: Seyfert – galaxies: starburst

1. Introduction

Emission-line galaxies form two main and distinct groups: the *broad-* and the *narrow-*emission-line galaxies, depending on the width of their permitted lines. The galaxies having intermediate line widths are the *intermediate* Seyfert galaxies 1.1 to 1.9.

The narrow-emission-line galaxies are particularly interesting, since they present the ambiguity to regroup under the same spectral characteristics two different types of galaxies: the H II galaxies (i.e. the starburst galaxies) and the narrow-emission-line AGNs (i.e. the Seyfert 2 galaxies and the LINERs).

The fundamental difference, which distinguishes these two types of galaxies, is based on the mechanism by which emission lines are produced. In the H II galaxies, the gas is photoionized by young, hot OB stars, whereas in the AGNs, the ionizing energy is supposed to come from accreting material around a supermassive black hole and the ionizing energy spectrum takes the form of power law continuum ($F_\nu \propto \nu^\alpha$).

The problem is now to recognize an AGN spectrum from a H II galaxy spectrum. *Spectral criteria*, other than the line width, that are able to accomplish this task are necessary and important for two main reasons: (1) of course, to distinguish the AGNs from H II galaxies in spectroscopic surveys of emission-line galaxies and (2) to separate, in high-resolution high signal to noise ratio (hereafter S/N) spectra of nuclear regions, the AGN component from the stellar one in galaxies presenting possible connections between starbursts and AGNs.

In this work, we re-examine the existing spectral criteria, based on line-ratios (Sect. 3), which are used to discriminate the AGNs from H II galaxies within the optical range. We look for new combinations of these different criteria in order to find a better classification method for narrow-emission-line galaxies. We effectively propose a new classification diagram involving the line ratios $R_{23} = ([\text{O II}] \lambda 3727 + [\text{O III}] \lambda 4959 + [\text{O III}] \lambda 5007) / \text{H}\beta$ and $[\text{O I}] \lambda 6300 / \text{H}\alpha$ (Sect. 5).

The data at our disposal for doing that is the “Spectrophotometric Catalogue of H II galaxies” (hereafter SCHG, Terlevich et al. 1991), which is first of all a H II galaxies catalogue, but where about 10% of AGNs have been included. We first re-classify (Sect. 4) all 800 spectra ($\lambda = 3600$ to 7800 \AA) of the catalogue in a different way than Terlevich et al. (1991) based only on the line-ratio diagram $[\text{O III}] / [\text{O II}]$ versus $[\text{O III}] / \text{H}\beta$, by using the three line-ratio diagrams of Veilleux & Osterbrock (Sect. 3.1) and by preliminary determining the broad-emission-line galaxies on the basis of Balmer’s lines width ($> 100 \text{ \AA}$).

Send offprint requests to: M. Dessauges-Zavadsky

Correspondence to: Miroslava.Zavadsky@obs.unige.ch

¹ Available in electronic form only via anonymous ftp 130.79.128.5 or <http://cdsweb.u-strasbg.fr/Abstract.html>

This re-classification allows us to establish a revised catalogue of the SCHG (see Table 3²) including H II galaxies, Seyfert 2 galaxies, LINERs and “intermediate” galaxies with “ambiguous” and “transition” galaxies (see Sect. 4.2). The resulting classification is compared with the one of the SCHG and with data available in the NASA/IPAC Extragalactic Database (hereafter NED).

2. Data description and spectral analysis

2.1. Data description

The data sample we are using in this work is composed of emission-line galaxies from the SCHG including about 10% of AGNs which will interest us particularly. Most objects in this catalogue have been selected from two sources: the Tololo survey (Smith et al. 1976) and the University of Michigan survey (MacAlpine & Lewis 1978; MacAlpine et al. 1977a, b, c; MacAlpine & Williams 1981). Both surveys were done with a thin objective prism on the 61 cm Curtis Schmidt telescope at Cerro Tololo.

The observations of the selected objects were obtained with different telescopes (3.6 m ESO telescope; 2.5 m Las Campanas telescope; 4.0 m Tololo telescope), with different slit widths (2 to 8 arcsec) and with different resolutions (ranging from about 10 to more than 20 Å). The spectral data we are using in this work are the data reduced by Terlevich et al. (1991). Their reductions were performed using the IHAP package at ESO and involved standard procedures for the correction of flat-field fluctuations, wavelength and flux calibrations.

Note that for the spectra taken at Las Campanas the fluxes above 6000 Å are underestimated (second order contamination, see Campbell et al. 1986 for more details), however this should not affect our analysis, since we will use only line-ratios with small wavelength separations.

With the aim of checking the homogeneity of the data and of improving the accuracy of the fluxes and of the line ratios, the catalogue of Terlevich et al. (1991) contains for many objects more than one observation. Thus, in total more than 800 spectra, ranging from $\lambda = 3600$ to 7800 Å, of 425 galaxies are present in the catalogue. The bulk of these galaxies have redshifts lower than $z = 0.05$, with a mean value near 0.02 and with some of them redshifted up to $z > 1$.

For their catalogue, Terlevich et al. (1991) aimed to observe only the central region of galaxies, and in fact their catalogue was originally made of what they called “H II region-like galaxies”. Most of these galaxies are compact, dominated by a central starburst. However a number of galaxies in the catalogue are spiral galaxies with H II region-like nuclei. For these galaxies, our classification may be affected by aperture effects, if the aperture used is larger than their nuclei. In this case, the observed [N II]/H α ratio, for instance, will be diluted, which could, if the

effect is severe, change their spectral classification (see e.g. Ho et al. 1993a and Storchi-Bergmann 1991 for more details).

2.2. Spectral analysis

The spectral analysis is the crucial point of this work, since galaxy classification depends on the measurements of emission-line intensity ratios. It is thus relevant to discuss in some details the method we used for re-measuring the line intensities.

The analysis was done with MIDAS package and piecemeal along the spectra in such a way that continuum could be fitted linearly. Once the continuum fit was determined, the line intensities were measured by visually placing the graphic cursor at both sides of each line where linewings became indistinguishable from the continuum, integrating then all the flux within that wavelength range minus the local continuum.

Emission-line measurements are easily obtained with high S/N for strong and isolated lines; the mean relative flux error goes from 5% for high S/N spectra to 15–20% for low S/N spectra. But things are more complicated for weak lines and particularly for blended lines which need a deblending procedure (fits of several Gaussians) for their intensity measurements.

The set of visible nebular lines present in most spectra of emission-line galaxies from the SCHG is (see Fig. 1):

$$\begin{aligned} [\text{O II}] \lambda &= 3727^3, [\text{Ne III}] \lambda = 3868, \text{H}\beta \lambda = 4861, \\ [\text{O III}] \lambda &= 4959, [\text{O III}] \lambda = 5007, [\text{O I}] \lambda = 6300, \\ [\text{N II}] \lambda &= 6548, \text{H}\alpha \lambda = 6563, [\text{N II}] \lambda = 6584, \\ [\text{S II}] \lambda\lambda &= 6717, 6731. \end{aligned}$$

A difficulty of intensity measurement is principally met for the lines [N II] λ 6548, H α and [N II] λ 6584 and the lines [S II] $\lambda\lambda$ 6717,6731 which are generally weak (except H α) and blended. As we only need the [N II] λ 6584 line intensity (three times brighter than the [N II] λ 6548 line), but with a rather good precision, we assumed that our measurement is correct when the position parameters of H α and [N II] λ 6584 lines obtained with the multi-fit corresponded to the theoretical ones by less than 2 Å (this criterion is equivalent to the one that would consist in taking only the spectra with sufficient resolution). The estimated mean relative flux error is of about 5–15% for H α and 15–25% for [N II] λ 6584.

In a general way, we decided to accept an intensity measurement of lines, such as [O I] λ 6300 or [S II] $\lambda\lambda$ 6717,6731 for instance, only when we obtained a relative flux error lower than 40% (especially for low S/N spectra).

The comparison of our intensity measurements (relative to H β) with those tabulated in Terlevich et al. (1991) for the most important lines ([O III] λ 5007, H α , [S II] $\lambda\lambda$ 6717,6731, [N II] λ 6584 and [O I] λ 6300) are in good agreement. Effectively the mean relative differences are correlated to the mean relative intensity errors estimated for these lines (which are themselves correlated to the S/N of spectra).

² The whole catalogue with our measurements of line intensities relative to H β is only available as Table 3 in electronic form at the CDS via anonymous ftp to cdsarc.u-strasbg.fr (130.79.128.5) or via http://cdsweb.u-strasbg.fr/Abstract.html.

³ Hereafter, [O II] λ 3727 represents the sum of the lines [O II] $\lambda\lambda$ 3726,3729.

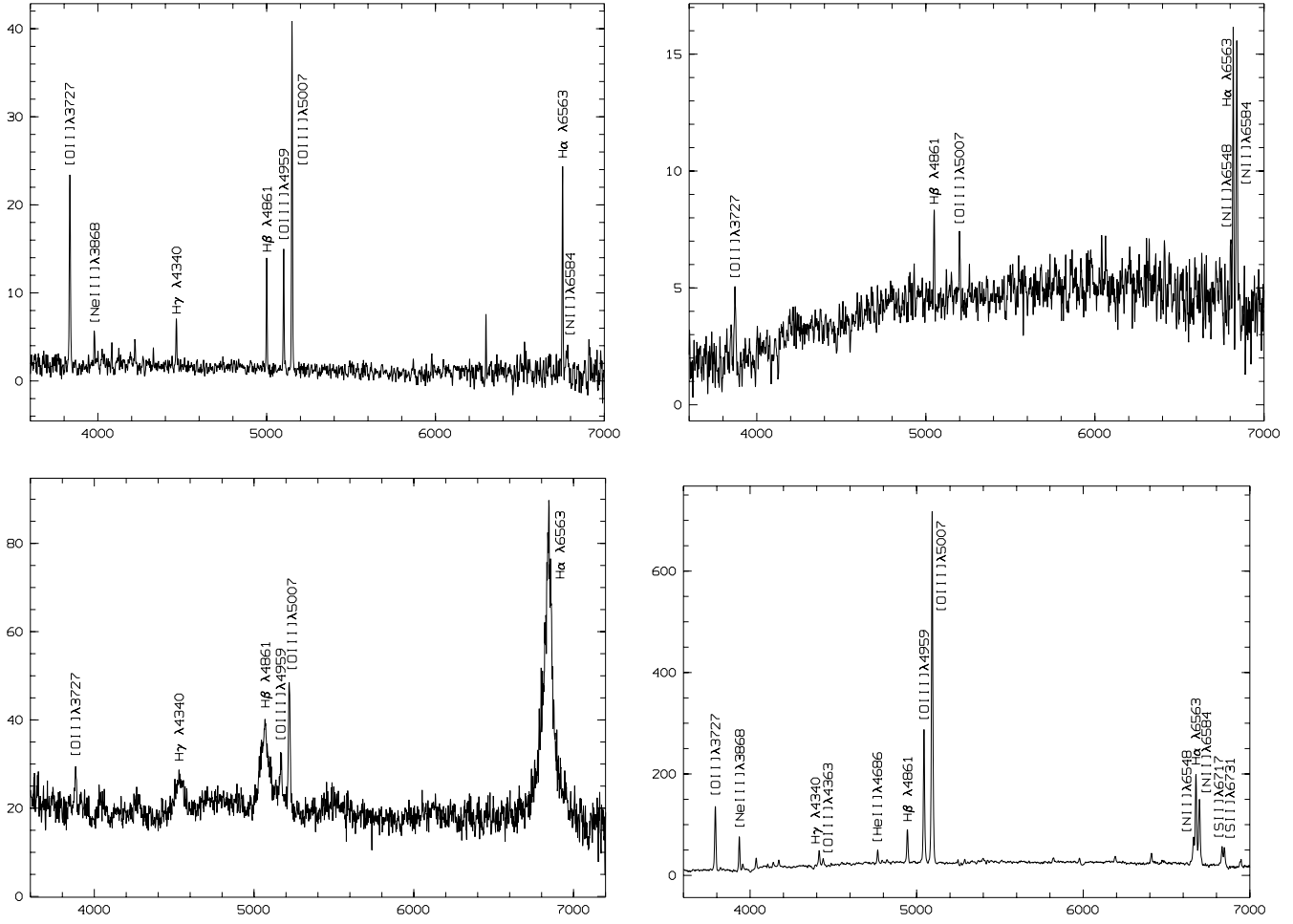


Fig. 1. Spectra of four types of emission-line galaxies (Terlevich et al. 1991): the H II galaxy Mich 159, the LINER galaxy Mich 11, the Seyfert 1 galaxy Tol 0343–397 and the Seyfert 2 galaxy Mich 363 (respectively from left to right and from up to down). The horizontal axes correspond to the observed wavelength in [\AA] and the vertical axes correspond to the flux in [$10^{-16} \text{ erg s}^{-1} \text{ cm}^{-2} \text{ \AA}^{-1}$].

2.3. Reddening corrections

There is no doubt for the presence of dust in H II regions galaxies and in Seyfert galaxies, nor that it modifies the spectra of these objects. However it is difficult to correct accurately for its extinction. Since very little is known about the properties of dust in these galaxies, the standard assumption is that the optical properties of dust in emission-line galaxies are identical to the optical properties of dust in our Galaxy.

The most widely method used to correct the emission-line spectra for the presence of dust is based on the relative strengths of lower Balmer lines. Usually the observed Balmer-line ratios are compared with the theoretical ones and the differences between them are assumed to be due to interstellar extinction (for a full description, see e.g. Osterbrock 1989).

In order to have an internally consistent sample, we applied the above method to each of our objects, using only the ratio of the two strongest Balmer lines, $H\alpha/H\beta$. Of course, for the spectra having second order contamination, the reddening estimated this way is wrong; that is why these spectra have not been taken into account when the effect of extinction on the

different diagnostic diagrams has been studied (see Sect. 4.1). For these strong Balmer lines, the stellar Balmer absorption has been neglected.

The effect of reddening on the ratio $H\alpha/H\beta$ can be written:

$$\frac{I(H\alpha)}{I(H\beta)} = \frac{F(H\alpha)}{F(H\beta)} \cdot e^{C_{H\beta} \cdot [f(H\alpha) - f(H\beta)]}, \quad (1)$$

where $C_{H\beta}$ is the measurement of the amount of reddening, $I(\lambda)$ is the intrinsic (unreddened) intensity and $F(\lambda)$ is the observed intensity. We used the reddening curve $f(\lambda)$ as parametrized by Izotov et al. (1994), so that $f(H\alpha) - f(H\beta) = -0.332$.

For the intrinsic intensity ratio for H II region-like objects, we adopted the Case B Balmer recombination decrement $I(H\alpha)/I(H\beta) = 2.85$ (Brocklehurst 1971) and for the intrinsic ratio for AGNs, $I(H\alpha)/I(H\beta) = 3.10$ is generally adopted (Ferland & Netzer 1983; Péquignot 1984). However since the nature of the studied objects (H II galaxy or AGN) is not *a priori* known and since the SCHG contains a majority of H II galaxies, the reddening corrections were computed only with the intrinsic intensity ratio $I(H\alpha)/I(H\beta) = 2.85$. The difference between 2.85 and 3.10 for AGNs is negligible.

3. Spectral classification of emission-line galaxies

3.1. Diagnostic diagrams of Veilleux & Osterbrock (1987)

The narrow-emission-line galaxies are generally classified by using the emission-line ratios of the most prominent lines. However AGNs cannot be distinguished from H II galaxies with a single parameter, thus classifications based on at least two line-intensity ratios are needed. The first authors to have developed such a method were Baldwin et al. (1981).

The search for the best line ratios for *two-dimensional classifications* of narrow-emission-line galaxies can be narrowed down by three criteria (Veilleux & Osterbrock 1987):

1. Each ratio should be made up of lines that are present and relatively easy to measure in typical spectra.
2. The wavelength separation between the two lines should be rather small so that the ratio is relatively insensitive to reddening and flux calibration.
3. Ratios involving a line of only one element and an H I Balmer line should be preferred to those involving forbidden lines of different elements because they are less abundance-sensitive.

The line ratios in the optical range that satisfy all three criteria are:

$$\begin{aligned} & [\text{O II}] \lambda 3727/\text{H}\beta; \\ & [\text{Ne III}] \lambda 3868/\text{H}\beta; \\ & [\text{O III}] \lambda 5007/\text{H}\beta \left(\longleftrightarrow [\text{O III}] (\lambda 4959 + \lambda 5007)/\text{H}\beta\right); \\ & [\text{O I}] \lambda 6300/\text{H}\alpha; \\ & [\text{N II}] \lambda 6584/\text{H}\alpha \left(\longleftrightarrow [\text{N II}] (\lambda 6548 + \lambda 6584)/\text{H}\alpha\right); \\ & [\text{S II}] (\lambda 6717 + \lambda 6731)/\text{H}\alpha. \end{aligned}$$

Different diagrams called *diagnostic diagrams* can be built from these line ratios, but certainly not all are very effective for distinguishing the AGNs from H II galaxies. The most famous diagnostic diagrams are those by Veilleux & Osterbrock (1987):

$$\begin{aligned} & \log [\text{O III}]/\text{H}\beta \text{ versus } \log [\text{S II}]/\text{H}\alpha \\ & \log [\text{O III}]/\text{H}\beta \text{ versus } \log [\text{N II}]/\text{H}\alpha \\ & \log [\text{O III}]/\text{H}\beta \text{ versus } \log [\text{O I}]/\text{H}\alpha \end{aligned}$$

The efficiency of these diagrams and the choice of these line ratios rest on the following effects (see Osterbrock 1989 for more details):

- The fundamental physical difference between an AGN and a H II galaxy is the photoionization mechanism. Thus, the presence of photons above 70 eV is negligible in H II galaxies which are photoionized by stars, but the energy of photons produced by power-law continuum in AGNs extends well beyond this value (X-ray photons). We can therefore assume that lines requiring ionizing potential higher than 70 eV are most likely produced by a power-law continuum rather than by unusually hot stars.
- The presence of photons of high energy has also important consequences for the ionization structure. As the photon

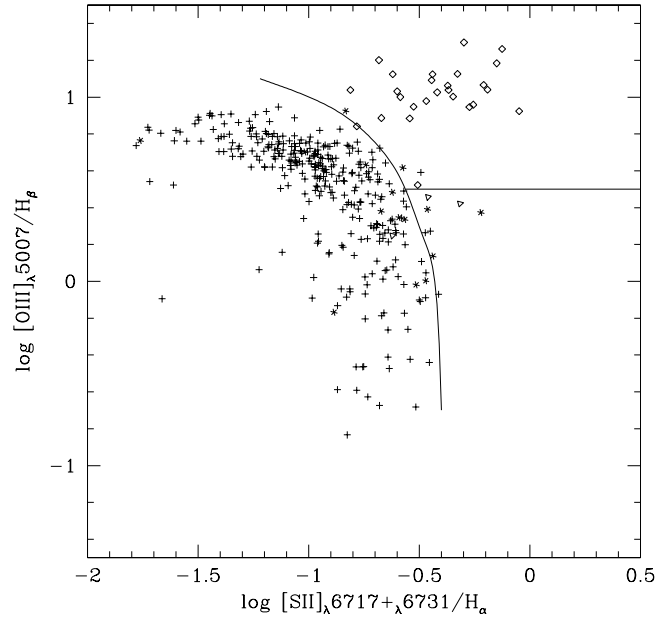


Fig. 2. Diagnostic diagram $\log [\text{O III}]/\text{H}\beta$ versus $\log [\text{S II}]/\text{H}\alpha$ of our sample of narrow-emission-line galaxies (without reddening corrections). The full lines correspond to the empirical separations between narrow-line AGNs and H II galaxies and between Seyfert 2 galaxies and LINERs, deduced by Veilleux & Osterbrock (1987) and Filippenko & Terlevich (1992) respectively. The crosses correspond to H II galaxies, the lozenges to Seyfert 2 galaxies, the triangles to LINERs and the stars to “intermediate” galaxies.

absorption cross sections of ions decrease rapidly with increasing photon energy, X-ray photons penetrate deeply into the predominantly neutral region. There they produce a large partially ionized H zone in which free electrons coexist with neutral atoms as well as with ions having a low ionization potential similar to the one of H. Lines such as [O I] $\lambda 6300$, [S II] $\lambda\lambda 6717, 6731$ and [N II] $\lambda 6584$ are produced in this zone. Such a partially ionized H zone also exists in H II regions photoionized by hot stars, i.e. by UV photons, but is clearly smaller.

- Finally, the ion O^{++} is produced predominantly by UV photons close to the ionizing source. The effect of the most energetic X-ray photons are not very important in that region. However, the relatively larger number of photons that can ionize O^+ to O^{++} in a power-law type spectrum generally makes the ratio $[\text{O III}] \lambda 5007/\text{H}\beta$ larger in the Seyfert 2 galaxies than in LINERs and H II galaxies.

As the intensities of low-ionization lines [O I] $\lambda 6300$, [S II] $\lambda\lambda 6717, 6731$ and [N II] $\lambda 6584$ with respect to $\text{H}\alpha$ are larger in narrow-line AGNs than in H II galaxies, we can now understand the efficiency of Veilleux & Osterbrock’s diagnostic diagram and the distribution of narrow-emission-line galaxies in these diagrams (see Figs. 2, 3, 4).

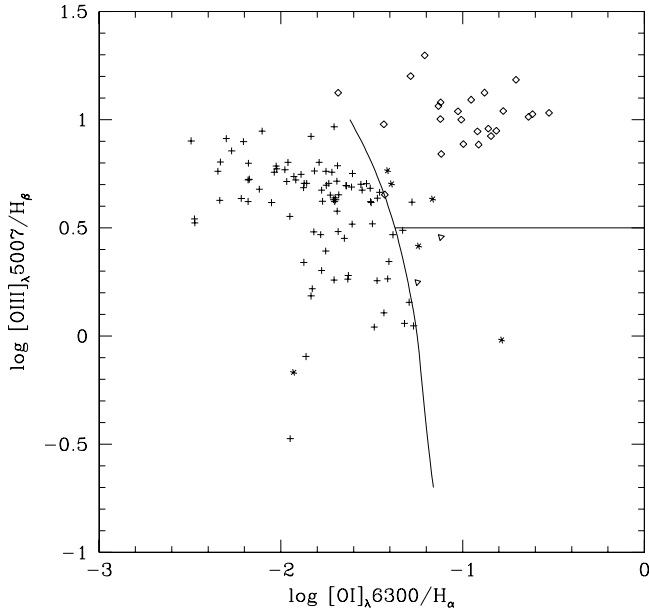


Fig. 3. Diagnostic diagram $\log [\text{O III}]/\text{H}\beta$ versus $\log [\text{O I}]/\text{H}\alpha$. See complementary remarks on Fig. 2.

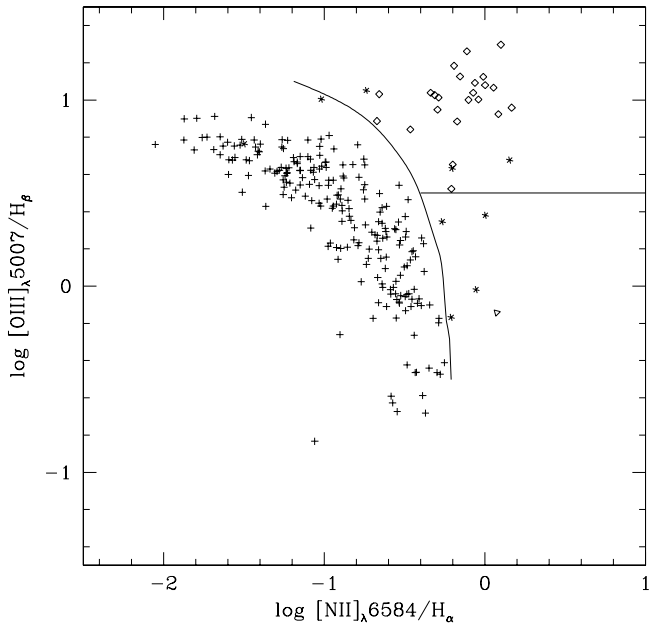


Fig. 4. Diagnostic diagram $\log [\text{O III}]/\text{H}\beta$ versus $\log [\text{N II}]/\text{H}\alpha$. See complementary remarks on Fig. 2.

3.2. Boundaries in the diagnostic diagrams of Veilleux & Osterbrock (1987)

The general idea of the distribution of narrow-emission-line galaxies in the diagnostic diagrams of Veilleux & Osterbrock (1987) is well understood and depends on the type of galaxies. However in order to separate completely these different types of galaxies (Seyfert 2 galaxies, LINERs, H II galaxies) we have to define boundaries between them. Theoretical boundaries between H II galaxies and narrow-line AGNs (see Radovich et al. 1998) can be determined by computing pho-

toionization models with, for instance, Ferland’s photoionization code CLOUDY 90 (Ferland 1996) or Rola’s photoionization code PHOTO (Rola 1995).

In this work, we have considered the *empirical boundaries* (see Figs. 2, 3, 4) defined by Veilleux & Osterbrock (1987) on the basis of a sample of narrow-emission-line galaxies which type (AGN or H II galaxy) was known and of the general shape of the boundary curves predicted by photoionization models.

Of course, the positions in the diagnostic diagrams of these boundary curves are not perfectly determined; this applies mainly to extremities of the curves. Thus, considering the uncertainties of the measured line-intensity ratios and of the positions of the boundary curves, the nature of any object within the “transition zones”, i.e. at ± 0.15 (value chosen by Veilleux & Osterbrock 1987) along these boundaries, is very difficult to determine. Such object, called “transition” object, may be either a pure H II galaxy or a pure narrow-line AGN (Heckman et al. 1983 and Keel et al. 1984). But it is also quite possible that both types of photoionization mechanisms are present in some objects. Another possibility is that the ionizing flux in the nuclei of these objects is caused by a central power-law source, while outside the nuclei ionization by hot stars is predominant.

Concerning the distinction between the narrow-line AGNs (Seyfert 2 galaxies and LINERs), another boundary has to be considered. An empirical boundary distinguishing these two types of AGNs has first been defined by Heckman (1980). It was based on the following criteria: $[\text{O II}] \lambda 3727/[\text{O III}] \lambda 5007 \geq 1$ and $[\text{O I}] \lambda 6300/[\text{O III}] \lambda 5007 \geq 1/3$ for the LINERs. Then another empirical boundary was proposed by Gonçalves et al. (1999) based on the parameter $\log [\text{O I}] \lambda 6300/[\text{O III}] \lambda 5007$ for more than 150 Seyfert 2 galaxies and LINERs. LINERs seem to have $\log [\text{O I}]/[\text{O III}] > 0.25$. Finally in 1992, Filippenko & Terlevich proposed on the basis of Heckman’s work the following empirical boundary:

$$\log [\text{O III}] \lambda 5007/\text{H}\beta \leq 0.5 \text{ for the LINERs.}$$

This boundary has the advantage to be directly applicable to the diagnostic diagrams of Veilleux & Osterbrock (1987).

4. Data classification

4.1. Classification method

The emission-line galaxies from the SCHG are re-classified in this work by using the different diagnostic diagrams of Veilleux & Osterbrock (1987) and their empirical boundaries separating the AGNs from H II galaxies and the Seyfert 2 galaxies from LINERs. As these diagnostic diagrams apply themselves only to *narrow-emission-line galaxies*, we must first determine in the sample of 800 spectra those containing broad permitted lines (essentially Balmer lines). These lines are the signatures of galaxies such as Seyfert 1 galaxies and intermediate Seyfert galaxies 1.1 to 1.5.

Because of their very large permitted line width ($\sim 130 \text{ \AA}$), Seyfert 1 galaxies (and intermediate ones) are easily recognizable (see Fig. 1), which is not the case for Seyfert 2 galaxies,

Table 1. Broad-emission-line galaxies

| Identity | Class |
|------------------|-------------|
| Mich 156 | Seyfert 1.5 |
| Mich 163 | Seyfert 1 |
| Mich 293 | Seyfert 1.5 |
| Mich 317 | Seyfert 1 |
| Mich 385 | Seyfert 1 |
| Mich 387 | Seyfert 1 |
| Mich 393 | Seyfert 1.5 |
| Mich 412 | Seyfert 1.2 |
| Mich 449 | Seyfert 1 |
| Mich 614 | Seyfert 1 |
| UM 472 | Seyfert 1 |
| Tol 0343-397 | Seyfert 1 |
| Tol 0349-406 | Seyfert 1 |
| Ward 1=ESO 198/G | Seyfert 1 |

LINERs and H II galaxies, having intrinsic line width lower than the spectral resolution ($\sim 15 \text{ \AA}$).

We obtained in total 14 broad-emission-line galaxies. They are listed in Table 1 and are composed of Seyfert 1 and intermediate Seyfert galaxies. The indicated nature for each of these galaxies is the one found in the NED.

The use of Veilleux & Osterbrock’s (1987) diagrams requires the intensity measurements of low-ionization lines [O I] $\lambda 6300$, [N II] $\lambda 6584$ and [S II] $\lambda\lambda 6717, 6731$. But as these measurements present some difficulties, all narrow-emission-line galaxies of Terlevich’s et al. (1991) catalogue cannot be classified with the diagnostic diagrams of Veilleux & Osterbrock (1987). Only 314 galaxies represented by 405 spectra from the initial 800 can be classified under our measurement selection criteria (see Sect. 2.2).

The diagnostic diagrams obtained without reddening corrections of intensity ratios are represented on Figs. 2, 3 and 4 with the H II galaxies on the left side and the narrow-line AGNs on the right side (Seyfert 2 galaxies up, LINERs down) as explained in Sect. 3.1. The bulk of H II galaxies is well separated from Seyfert 2 galaxies.

To check the effect of reddening on the intensity ratios used in the diagnostic diagrams of Veilleux & Osterbrock (1987), we compared the values of the intensity ratios corrected for reddening according to Sect. 2.3 with the non-corrected ones (only for the spectra without second order contamination). We concluded from this comparison (not plotted in this paper) that the reddening effect on the intensity ratios is weak (less than 10%), since the lines of these ratios have small wavelength separations. Thus, one can admit that the reddening does not influence the classification of emission-line galaxies outside of zones close to boundaries.

4.2. Narrow-emission-line galaxies

The diagnostic diagrams (Figs. 2, 3, 4) allow us to establish a revised classification of narrow-emission-line galaxies from the SCHG. All H II galaxies (see Table 3) will not be enumerated,

Table 2. Narrow-emission-line galaxies

| Seyfert 2 | LINER | “Intermediate” | “Revised” |
|--------------|------------|----------------|-----------|
| Fairall 4 | Mich 11* | Mrk 632 | Mich 146* |
| Fairall 21 | 0902+1448 | Mich 13* | Mich 147* |
| Mrk 1193 | 1204+1023* | Mich 480* | Mich 488 |
| Mrk 1210 | | Mich 539* | NGC 2989 |
| Mich 16 | | Mich 564* | |
| Mich 82 | | NGC 1614 | |
| Mich 85 | | NGC 1672 | |
| Mich 103 | | NGC 3089 | |
| Mich 105 | | Tol 0003-402* | |
| Mich 319 | | Tol 0124-413* | |
| Mich 363 | | Tol 0145-391* | |
| Mich 428 | | Tol 0452-415* | |
| Mich 625 | | Tol 0527-394* | |
| NGC 1386 | | Tol 1257-399* | |
| NGC 2089 | | Tol 2122-408 | |
| NGC 3081 | | | |
| NGC 3281 | | | |
| NGC 4507 | | | |
| Tol 0514-415 | | | |
| Tol 0544-395 | | | |
| Tol 0611-379 | | | |
| Tol 1124-289 | | | |
| Tol 1313-309 | | | |
| Tol 1345-419 | | | |
| 14-00 F 51 | | | |

* Galaxies classified with only *one* diagnostic diagram.

since our interest will particularly go towards the narrow-line AGNs (Seyfert 2 galaxies and LINERs) and towards galaxies for which the classification AGN/H II galaxy is uncertain. Each determined type of any object will be compared to the type deduced by Terlevich et al. (1991) and to the one available in the NED.

To determine the final classification of our sample of 314 galaxies, we have first considered the classification derived from each diagnostic diagram and then analysed the balance of these three classifications. Of course, we were not able to measure all the three low ionization lines ([O I] $\lambda 6300$, [N II] $\lambda 6584$ and [S II] $\lambda\lambda 6717, 6731$) for each galaxy. Thus, some galaxies have been classified using three diagnostic diagrams (55 of them) and others using only one (122 of them) or two diagrams (137 of them). The classification of objects present in only *one* diagnostic diagram is more tricky, so these objects are annotated by an asterisk in Table 2.

Then we have established a set of cross-check criteria between the balance of the three classifications and the classification given by Terlevich et al. (1991) and the one found in the NED. These criteria lead us to define three particular classes of objects:

1. The class of “revised” objects which classification is in contradiction with the one indicated by Terlevich et al. (1991) or found in the NED.

2. The class of “transition” objects located at about ± 0.15 from empirical boundaries in the diagnostic diagrams of Veilleux & Osterbrock (1987).
3. The class of “ambiguous” objects classified both as AGNs and H II galaxies in different diagnostic diagrams of Veilleux & Osterbrock (1987).

The results of our classification are summarized in Table 2 and are represented on Figs. 2, 3 and 4 using different symbols. From the sample of 314 narrow-emission-line galaxies, our classification leads us to determine a catalogue containing 267 H II galaxies (i.e. 84%), 25 Seyfert 2 galaxies (i.e. 8%), 3 LINERs (i.e. 1%), 4 “revised” galaxies (i.e. 2%) and 15 “intermediate” galaxies (i.e. 5%).

Among the 4 “revised” objects, one finds: Mich 147 (classified as a Seyfert 2 galaxy) disagreeing with Terlevich’s et al. (1991) classification (classified as a H II galaxy); Mich 488 (classified as a H II galaxy) and NGC 2989 (classified as a Seyfert 2 galaxy) disagreeing with the classification found in the NED (Seyfert 2 and H II galaxy respectively); and Mich 146 (classified as a H II galaxy) disagreeing with both the classification found in the NED and given by Terlevich et al. (1991) (Seyfert 2 galaxy for both). Note that Mich 146 and Mich 147 have been classified using only one diagnostic diagram.

And among the 15 “intermediate” objects, one finds:

- 13 “transition” objects with 9 of them classified as H II galaxies by Terlevich et al. (1991), the four others are not classified neither by Terlevich et al. (1991) nor in the NED.
- 2 “ambiguous” objects with Mrk 632 classified as a H II galaxy by Terlevich et al. (1991) and NGC 1672 classified as a Seyfert 2 galaxy in the NED (see references therein).

The “ambiguous” galaxies are particularly interesting in the sense that they present a real contradiction between the different classifications obtained from diagnostic diagrams. But we must be careful, for two reasons, before making any hasty conclusion about these objects: (1) they can simply belong to this class because of the bad quality of their spectra rather than their nature; our two defined “ambiguous” galaxies have effectively spectra contaminated by an underlying old stellar population; and (2) the aperture effects mentioned in Sect. 2.1 could also be a cause for “ambiguous” objects as well as for “transition” objects, in some cases (see Ho et al. 1993a). Nevertheless note that the “ambiguous” and “transition” galaxies are not systematically more redshifted than the rest of the galaxies, and thus their distance seems not to be responsible for any particular aperture effect. However, this sub-sample is not large enough to make any statistical conclusion.

If we look for physical reasons explaining the difficulty to classify some narrow-line objects (see Gonçalves et al. 1999 and Véron et al. 1997 for some other examples of “intermediate” galaxies), one can recall the three hypothesis mentioned by Rola et al. (1997): (1) these objects are in fact *composite* objects (H II/AGN) with an AGN component weaker or stronger than the emission component produced from ionization by stellar sources; (2) they are H II galaxies with a peculiar “hot” stellar

population; and (3) these objects have just different properties in their ionized regions. Future work will have to be led to determine what makes these objects really different from AGNs or H II galaxies.

5. Known and new diagnostic diagrams

On the basis of the revised Terlevich et al. (1991) catalogue (see Sect. 4.2), we have investigated a research for some new diagnostic diagrams constructed from different combinations of the set of the most prominent optical nebular lines (see Sect. 2.2). Only the most interesting diagrams obtained for the classification of H II galaxies and narrow-line AGNs will be presented.

5.1. Rola et al. (1997) diagnostic diagrams

We begin this section by first considering the diagrams of Rola et al. (1997). These diagrams have been proposed because of the recent need to classify spectra of redshifted galaxies. The nearby narrow-line galaxies are classified using the emission-line ratios of optical lines, like [O I] $\lambda 6300$, [O III] $\lambda 5007$, [N II] $\lambda 6584$, [S II] $\lambda \lambda 6717, 6731$, H α and H β (see Sect. 3). But in higher redshifted objects ($z > 0.3$), most of these lines move out of the observable optical spectral range. It is therefore important to be able to determine the nature of redshifted narrow-emission-line galaxies independently of reddening and using a minimum of emission lines between [O II] $\lambda 3727$ and [O III] $\lambda 5007$ observable in the optical range up to $z \approx 0.75$.

Rola et al. (1997) investigated a diagnostic diagram using the [O II] $\lambda 3727$, [Ne III] $\lambda 3868$, H β and [O III] $\lambda 5007$ emission lines and not requiring reddening or stellar absorption corrections:

$$\log [\text{Ne III}] \lambda 3868/\text{H}\beta \text{ versus } \log [\text{O II}] \lambda 3727/\text{H}\beta.$$

We wished to check the efficiency of this diagram to distinguish the narrow-line AGNs from H II galaxies thanks to our sample of classified narrow-emission-line galaxies defined in the Sect. 4.2. And as we can see it on Fig. 5, this diagram is effectively quite efficient in separating the AGNs from H II galaxies. We can estimate an empirical limit situated at $\log [\text{Ne III}] \lambda 3868/\text{H}\beta \approx -0.2$ above which about 75% of Seyfert 2 galaxies are located. The same limit was determined by Rola et al. (1997) from a completely different sample of narrow-emission-line galaxies.

This diagram and the estimated empirical limit allow to separate the Seyfert 2 from H II galaxies, but the separation between the LINERs and these two types of galaxies remains undefined. A complementary diagram involving the intensity ratio [O III] $\lambda 5007/\text{H}\beta$ (see Fig. 6), as proposed by Rola et al. (1997), allows some level of segregation between LINERs ($\log [\text{O III}] \lambda 5007/\text{H}\beta < 0.5$) and Seyfert 2 galaxies ($\log [\text{O III}] \lambda 5007/\text{H}\beta > 0.5$) (but not between LINERs and H II galaxies). However we cannot analyse the behaviour of LINERs in this diagram, since the SCHG contains only 3 LINERs

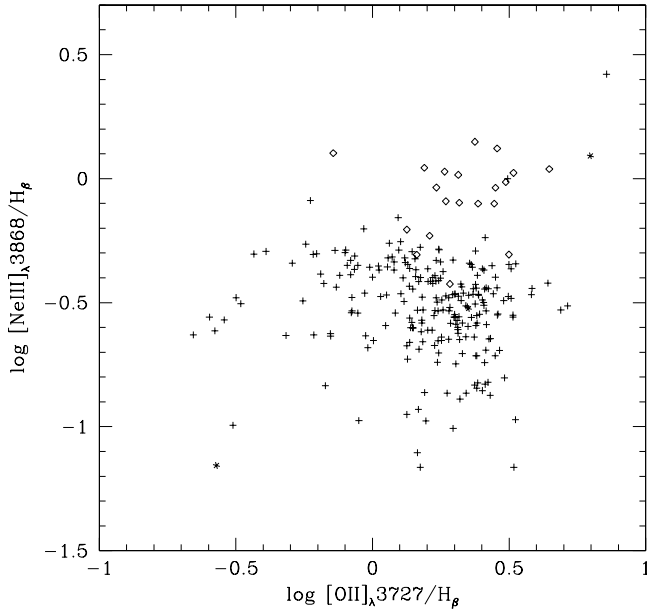


Fig. 5. Diagnostic diagram of Rola et al. (1997) of our sample of classified narrow-emission-line galaxies (without reddening corrections). Symbols same as in Fig. 2.

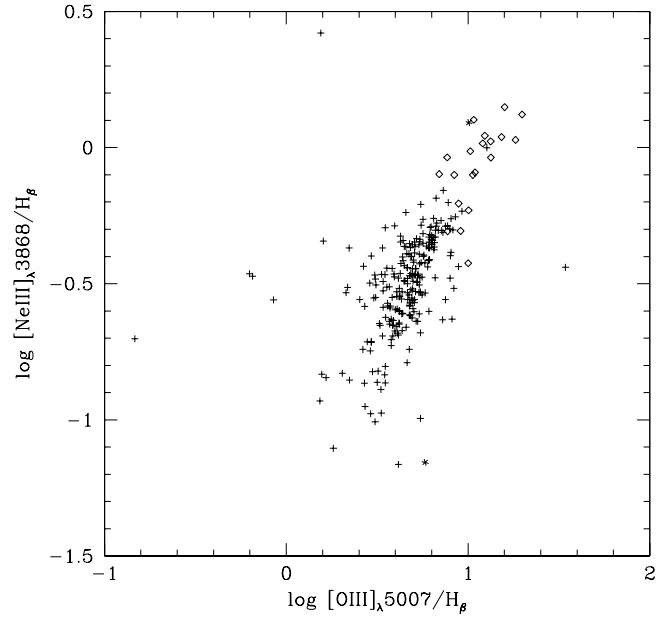


Fig. 6. Diagnostic diagram of Rola et al. (1997) of our sample of classified narrow-emission-line galaxies (without reddening corrections). Symbols same as in Fig. 2.

(see Sect. 4.2) and since a precise enough measurement of the [Ne III] $\lambda 3868$ line could not be done for them.

The difficulty of measuring the [O II] $\lambda 3727$ and [Ne III] $\lambda 3868$ lines, because of their position in the spectra (near the blue limit at about $\lambda=3600$ Å), explains also why Figs. 5 and 6 contain only 2 “intermediate” galaxies. From 405 classified spectra, only 240 have a good enough S/N allowing a correct measurement of both [O II] $\lambda 3727$ and [Ne III] $\lambda 3868$ lines.

5.2. New diagnostic diagrams

In a similar method as the one used by Veilleux & Osterbrock (1987) and Rola et al. (1997), we have examined the possibilities of optimizing the separation between the AGNs and the H II galaxies. That is why we have constructed different additional diagnostic diagrams from (1) low-ionization emission lines ([O I] $\lambda 6300$, [N II] $\lambda 6584$, [S II] $\lambda\lambda 6717, 6731$), (2) oxygen lines ([O I] $\lambda 6300$, [O II] $\lambda 3727$, [O III] $\lambda 5007$) and (3) the intensity ratio R_{23} (see below), using our sample of classified narrow-emission-line galaxies (see Sect. 4.2). We will only present the diagram involving the intensity ratio R_{23} , since the other diagrams⁴ do not allow to make a better distinction be-

tween the narrow-line AGNs and the H II galaxies than the “traditional” diagnostic diagrams of Veilleux & Osterbrock (1987).

The emission-line ratio R_{23} is defined as:

$$R_{23} = ([\text{O II}] \lambda 3727 + [\text{O III}] \lambda 4959 + [\text{O III}] \lambda 5007) / \text{H}\beta$$

and it is usually used to estimate the O/H abundance ratio. The idea is here to use this intensity ratio for distinguishing the AGNs from H II galaxies. Using R_{23} can be justified by the following reasons. First, as it can be remarked from Veilleux & Osterbrock’s diagnostic diagrams (see Figs. 2, 3, 4), the values of the intensity ratio [O III] $\lambda 5007/\text{H}\beta$ are for the majority of Seyfert 2 galaxies higher compared to those of LINERs and H II galaxies. Secondly, the mean value of the intensity ratio [O II] $\lambda 3727/\text{H}\beta$ is also slightly higher for the Seyfert 2 galaxies than for the H II galaxies as it is seen on Figs. 5 and 7 where is plotted the diagram $\log [\text{O III}]/\text{H}\beta$ versus $\log [\text{O II}]/\text{H}\beta$ used by Tresse et al. (1996) as a diagnostic diagram. Thus, the intensity ratio R_{23} which is the resultant of these distinct contributions should be higher in the Seyfert 2 galaxies than in the H II galaxies.

We have constructed the $\log R_{23}$ versus $\log [\text{O I}] \lambda 6300/\text{H}\alpha$ diagram (Fig. 8), where the choice of the [O I] $\lambda 6300/\text{H}\alpha$ ratio is justified by the fact that the separation between the two classes of objects (AGNs and H II galaxies) is more distinct in Veilleux & Osterbrock’s (1987) diagram involving the [O I] $\lambda 6300/\text{H}\alpha$ line (see Figs. 2, 3, 4). Fig. 8 shows an interesting result relatively to the diagrams constructed from the [O III] $\lambda 5007/\text{H}\beta$ ratio. The separation between the Seyfert 2 galaxies and the H II galaxies is really well defined by the ratio R_{23} and we can remark that the Seyfert 2 galaxies dominate effectively the top of the diagram and the H II galaxies the bottom, as supposed. An empirical limit is estimated at $\log R_{23} \approx 1.1$ above which around 87% of Seyfert 2 galaxies are located.

⁴ We have analysed the following diagrams:

$\log [\text{S II}]/\text{H}\alpha$ versus $\log [\text{O I}]/\text{H}\alpha$;
 $\log [\text{S II}]/\text{H}\alpha$ versus $\log [\text{N II}]/\text{H}\alpha$;
 $\log [\text{N II}]/\text{H}\alpha$ versus $\log [\text{O I}]/\text{H}\alpha$;
 $\log [\text{O II}]/\text{H}\beta$ versus $\log [\text{O I}]/\text{H}\alpha$;
 $([\text{O III}]/\text{H}\beta - [\text{O II}]/\text{H}\beta)$ versus $([\text{O II}]/\text{H}\beta - [\text{O I}]/\text{H}\alpha)$;
 $\log [\text{O I}]/\text{H}\alpha$ versus $\log [\text{O II}]/[\text{O III}]$;
and $\log [\text{N II}]/\text{H}\alpha$ versus $\log [\text{O II}]/[\text{O III}]$.

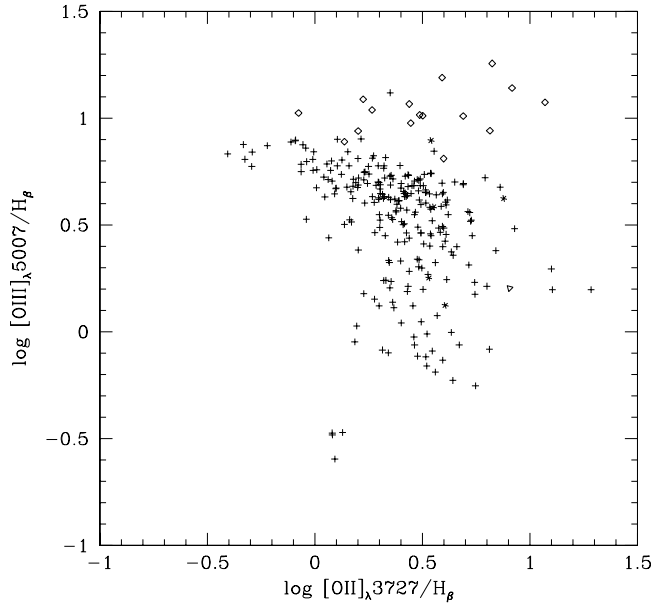


Fig. 7. Diagram $\log [\text{O III}]/\text{H}\beta$ versus $\log [\text{O II}]/\text{H}\beta$ of our sample of classified narrow-emission-line galaxies (without reddening corrections). This diagram was used by Tresse et al. (1996) as a diagnostic diagram. Symbols same as in Fig. 2.

Consequently the principal advantage of such a diagnostic diagram involving the R_{23} ratio relatively to the Veilleux & Osterbrock’s (1987) diagnostic diagrams is that it allows to make a better and an easier separation between the Seyfert 2 galaxies and the H II galaxies. Thus, the cases of “transition” galaxies could be reduced.

The difficulty of measuring both $[\text{O II}] \lambda 3727$ and $[\text{O I}] \lambda 6300$ lines prevents us from observing the position of LINERs and “intermediate” galaxies from the SCHG in the new diagram. Effectively, from 405 classified spectra, only 76 have a good enough S/N allowing a correct measurement of these two lines⁵. To complete the catalogue of Terlevich et al. (1991), containing only 3 LINERs, we took 9 LINERs studied by Ho et al. (1993b) and placed them in the diagram (solid triangles). We can see a clear separation between these LINERs and the Seyfert 2 galaxies as well as the H II galaxies, and we can remark that the empirical limit $\log R_{23} \approx 1.1$ allows also to distinguish the Seyfert 2 galaxies from LINERs.

Nevertheless this empirical limit is not sufficient to separate the narrow-line AGNs from H II galaxies. But a theoretical limit separating the AGNs from H II galaxies can be constructed with the help of photoionization models in the same way as in Veilleux & Osterbrock’s diagnostic diagrams. Especially since the intensity ratio R_{23} is linked with the intensity ratio $[\text{O III}] \lambda 5007/\text{H}\beta$ (see Fig. 9) and consequently with the

⁵ However the limit $\log R_{23} \approx 1.1$ estimated for separating the Seyfert 2 galaxies from H II galaxies remains interesting not only for this small sample of 76 spectra, but for the whole sample of spectra (representing a total of 240) for which a good measurement of the ratio R_{23} (mean relative flux error < 20%), i.e. of the line $[\text{O II}] \lambda 3727$, is possible.

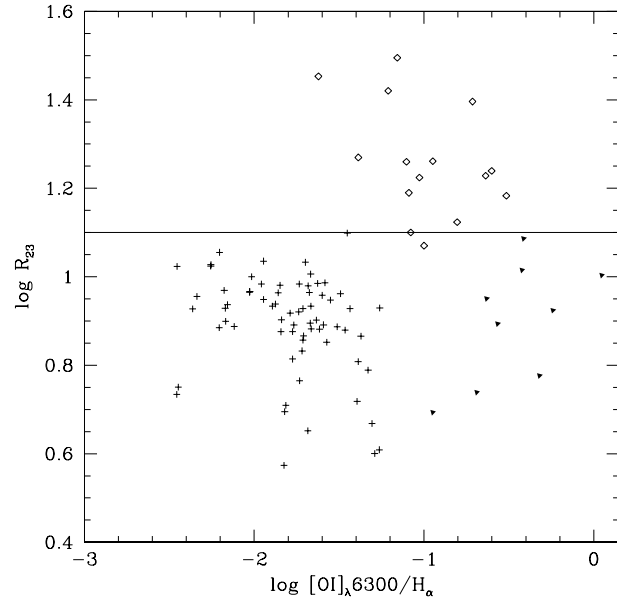


Fig. 8. Proposition of a new diagnostic diagram of our sample of classified narrow-emission-line galaxies (with reddening corrections). The full line corresponds to the empirical separation between H II galaxies and Seyfert 2 galaxies. Symbols same as in Fig. 2 with solid triangles corresponding to LINERs from Ho et al. (1993b).

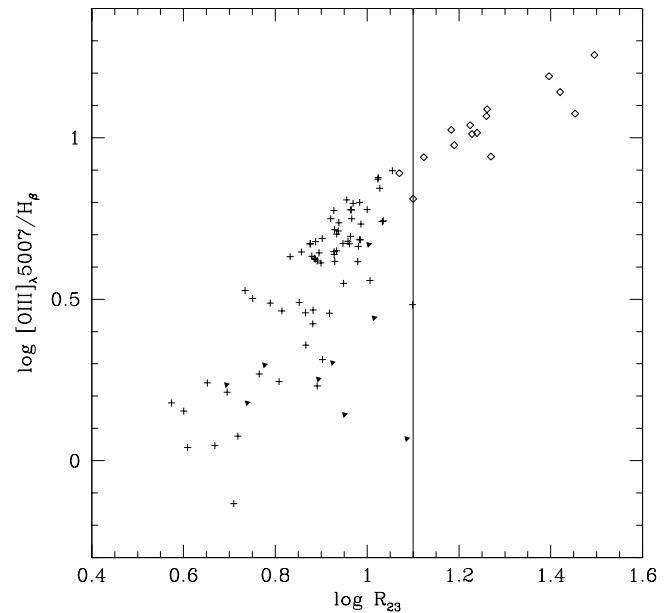


Fig. 9. Diagram showing the relation between the intensity ratios $[\text{O III}]/\text{H}\beta$ and R_{23} of our sample of classified galaxies (with reddening corrections). See complementary remarks on Fig. 8.

ionization parameter (Radovich et al. 1998). Note that this last diagram could be used to separate the Seyfert 2 from both H II galaxies and LINERs for objects having intermediate redshifts (up to $z \approx 0.75$), since it is constructed from emission lines between $[\text{O II}] \lambda 3727$ and $[\text{O III}] \lambda 5007$, as in the diagrams of Rola et al. (1997).

6. Conclusion

The main goal of this work was to re-classify (in a different way than the one used by Terlevich et al. 1991) the emission-line galaxies of their catalogue in order to obtain a revised and checked catalogue of a sample of narrow-emission-line galaxies. The classification was realized thanks to the diagnostic diagrams of Veilleux & Osterbrock (1987) and to a determination of broad-emission-line galaxies based on a simple measurement of Balmer's lines width ($\geq 100 \text{ \AA}$). The comparison of our classification with that from Terlevich et al. (1991) and the one available in the NED allows us to reach our goal and to define a revised catalogue of the studied narrow-emission-line galaxies (see Table 3): H II galaxies, Seyfert 2 galaxies, LINERs, "revised" galaxies and "intermediate" galaxies (including "transition" and "ambiguous" galaxies).

The two galaxies classified as "ambiguous" because of the difficulty to determine their nature (narrow-line AGN or H II galaxy) constitute particularly interesting candidates for a study of connections between starbursts and AGNs. Therefore one could be thinking of doing a thorough study of these galaxies either on the basis of an integrated spectrum with an important signal to noise in the same way as was made the study of Mrk 477 by Heckman et al. (1997) or the study of NGC 5252 by Gonçalves et al. (1998), or on the basis of a spatially resolved spectra (integral spectroscopy) of central regions of these galaxies.

The establishment of the revised SCHG allows us to undertake a search for new diagnostic diagrams. We have been able to confirm the efficiency of diagrams proposed by Rola et al. (1997) which are particularly interesting for the classification of galaxies having redshifts up to ≈ 0.75 . We have also proposed some new diagnostic diagrams, constructed with lines in the optical range, among which the diagram

$$\log R_{23} \text{ versus } \log [\text{O I}] \lambda 6300/\text{H}\alpha$$

has hold our attention. The emission-line intensity ratio $R_{23} = ([\text{O II}] \lambda 3727 + [\text{O III}] \lambda 4959 + [\text{O III}] \lambda 5007) / \text{H}\beta$ seems effectively to be a very interesting criterion allowing to make a better discrimination between the Seyfert 2 and both the H II galaxies and the LINERs, relatively to the intensity ratio $[\text{O III}] \lambda 5007 / \text{H}\beta$ used in the diagnostic diagrams of Veilleux & Osterbrock (1987).

Acknowledgements. This work has made use of the "Spectrophotometric Catalogue of H II galaxies" by Terlevich et al. (1991). We therefore extend our thanks to R. Terlevich for granting us access to the data of his catalogue. We also thank L. Martinet, D. Friedli for most helpful discussions and A. C. Gonçalves for most useful advices.

References

- Baldwin J.A., Phillips M.M., Terlevich R.J., 1981, PASP 93, 5
 Brocklehurst M., 1971, MNRAS 153, 471
 Campbell A., Terlevich R.J., Melnick J., 1986, MNRAS 223, 811
 Ferland G.J., 1996, A brief introduction to Cloudy, Univ. of Kentucky, Dpt. of Physics and Astronomy, Internal Report
 Ferland G.J., Netzer H., 1983, ApJ 264, 105
 Filippenko V.A., Terlevich R.J., 1992, ApJ 397, L79
 Gonçalves A.C., Véron-Cetty M.-P., Véron P., 1999, A&AS 135, 437
 Gonçalves A.C., Véron P., Véron-Cetty M.-P., 1998, A&A 333, 877
 Heckman T.M., Gonzalez-Delgado R., Leitherer C., et al., 1997, ApJ 482, 114
 Heckman T.M., van Breugel W., Miley G.K., Butcher H.R., 1983, AJ 88, 1077
 Heckman T.M., 1980, A&A 87, 152
 Ho L.C., Shield J.C., Filippenko A.V., 1993a, ApJ 410, 567
 Ho L.C., Filippenko A.V., Sargent W.L.W., 1993b, ApJ 417, 63
 Izotov Y.I., Thuan T.X., Lipovetsky V.A., 1994, ApJ 435, 647
 Keel W.C., 1984, ApJ 282, 75
 MacAlpine G.M., William G.A., 1981, ApJS 45, 113
 MacAlpine G.M., Lewis D.W., 1978, ApJS 36, 587
 MacAlpine G.M., Lewis D.W., Smith S.B., 1977a, ApJS 35, 203
 MacAlpine G.M., Smith S.B., Lewis D.W., 1977b, ApJS 34, 95
 MacAlpine G.M., Smith S.B., Lewis D.W., 1977c, ApJS 35, 197
 Osterbrock D.E., 1989, Astrophysics of Gaseous Nebulae and Active Galactic Nuclei
 Péquignot D., 1984, A&A 131, 159
 Radovich M., Hafinger G., Rafanelli P., 1998, Astron. Nachr. 319–6, 325
 Rola C.S., Terlevich E., Terlevich R.J., 1997, MNRAS 289, 419
 Rola C.S., 1995, PhD Thesis, Université de Paris VII, France
 Smith M.G., Aguirre C., Zelman M., 1976, ApJS 32, 217
 Storchi-Bergmann T., 1991, MNRAS 249, 404
 Terlevich R.J., Melnick J., Masegosa J., Moles M., Copetti M.V.F., 1991, A&AS 91, 285
 Tresse L., Rola C.S., Hammer F., et al., 1996, MNRAS 281, 847
 Veilleux S., Osterbrock D.E., 1987, ApJS 63, 295
 Véron P., Gonçalves A.C., Véron-Cetty M.-P., 1997, A&A 319, 52